IOPscience iopscience.iop.org

Home Search Collections Journals About Contact us My IOPscience

Driven diffusion in solid media: a matrix formalism

This article has been downloaded from IOPscience. Please scroll down to see the full text article.

2009 J. Phys. A: Math. Theor. 42 055201

(http://iopscience.iop.org/1751-8121/42/5/055201)

View the table of contents for this issue, or go to the journal homepage for more

Download details:
IP Address: 171.66.16.156
The article was downloaded on 03/06/2010 at 08:27

Please note that terms and conditions apply.

IOP PUBLISHING JOURNAL OF PHYSICS A: MATHEMATICAL AND THEORETICAL

J. Phys. A: Math. Theor. **42** (2009) 055201 (19pp) doi:10.1088/1751-8113/42/5/055201

Driven diffusion in solid media: a matrix formalism

Roger Bidaux[1] **and Joseph Kolibal**[2]

[1] SPEC (CNRS URA 2464), CEA Saclay, BP 2, 91191 Gif-sur-Yvette, France
[2] Department of Mathematics, The University of Southern Mississippi, Hattiesburg, MS 39406, USA

Received 16 June 2008, in final form 22 October 2008
Published 6 January 2009
Online at stacks.iop.org/JPhysA/42/055201

Abstract
We develop a model of driven diffusion using a lattice approach in which the site-to-site pathways through the medium are represented as edges in a graph connecting vertices representing the medium. The movement of particles is accomplished using a column stochastic matrix to advance the state of the system. The method has computational advantages relative to Monte Carlo, and is less difficult to implement than continuum methods. Moreover, the formulation allows for the analytical computation of mean crossing times, which in turn shows that there are optimal values of the bias that lead to minimal mean crossing times.

PACS numbers: 82.56.Lz, 87.15.Vv, 05.40.Fb, 07.05.Tp

1. Introduction

Driven diffusion is taken to mean a diffusion process into which a bias is introduced, yielding a statistical preference for privileged directions or paths, thereby altering the symmetry of the process. In purely physical phenomena related to driven diffusion, the symmetry breaking factor may be an applied electric or magnetic field, such as in electrophoresis; a pressure, extracting a liquid from a solid material where it has been absorbed by spinning or compressing the material; or an attractive or repulsive device which causes the diffusing agents to move preferably toward or away from the device. In some cases, the cause of anisotropy is intrinsic to the medium and dispersed therein, such as heterogeneities of chemical potential creating gatherings of particles [1, 2]. Finally, the anomalous diffusion may be that of a thermal packet [3].

The primary interest of this study is in the use of a matrix formalism to obtain analytical estimates of the mean crossing time, and to demonstrate the utility of this approach in parametric studies applied to problems involving driven diffusion. While complex Monte Carlo methods are required to model these transport processes in detail, particularly time-dependent ones, they are computationally expensive and time consuming to develop. In contrast to Monte Carlo models for driven diffusion through a medium [4], using a stochastic

 © 2009 IOP Publishing Ltd Printed in the UK

lattice model may have significant computational advantages, particularly when studying heterogeneous materials such as nano-composites [5].

In the stochastic lattice model that is developed, the transport pathways through the medium are modeled using a graph in which edges connect nodes representing accessible sites. These nodes discretize the position of the particles at each time level, so that time itself is parametrized as an index. Particles move through the medium without interacting with each other, although this possibility is also considered in the formalism that is developed in section 4. Obstacles to the particles' movement are modeled using impurities that change the porosity of the medium. In particular, some nodes may be inaccessible, i.e., the lattice may contain edge–path obstructions, that may combine to either partially, or totally obstruct the local movement of particles through the grid. The motion of the particle through the medium is given by a probabilistic rule-set containing a directional bias, thus ensuring an overall statistical displacement of the particle in a preferred direction. The particle densities are then re-distributed at the lattice nodes using a probabilistic model to describe the transition of the system in time.

Using a matrix formalism to model these driven diffusion problems provides an analytical form for the expectation of the crossing time $\langle T \rangle$, and its standard deviation. The results show that, for a sample of given size, for a given concentration of impurities, there is an optimal choice of the bias parameter that makes $\langle T \rangle$ the smallest possible. Subsequently, a heuristic method is proposed to deal with the case of many particles, and a discussion of the defects and merits of the matrix method, along with possible extensions or variations on the method is provided. While a variety of diffusion and random walk problems have been examined in [6–8], including the use of analytical approaches to reduce the complexity of the modeling problem, these do not directly address the mean crossing time problem discussed in this paper.

2. Modeling considerations

2.1. Background

In its standard formulation, driven diffusion requires the following ingredients: (1) a particle or particles; (2) a hosting medium in which these particles propagate; and (3) an anisotropic displacement of the particles through the medium. The transport mechanism is modeled using a graph representing the medium through which the particle's motion is represented using node-to-node transition probabilities associated with the edges of the graph.

These transition probabilities yield a stochastic matrix, S, which describes the transition from one state, or time level, to the next state, or time level, of the system. Thus given an initial state vector $\mathbf{v}^0 = \left[v_0^0, v_1^0, \ldots, v_N^0\right]$ describing the distribution of the particles at some initial time at each accessible node, $i = 1, 2, \ldots, N$, in the graph of the lattice, the particle distribution at time step k is given by

$$\mathbf{v}^k = SS \cdots SV^0 = S^k \mathbf{v}^0. \tag{1}$$

The nodal transitions can be predicted through the use of molecular simulations, requiring an inner-iteration computational loop to assign these probabilities. In this approach the matrix S itself may be changing with each iteration, and thus the state of the system is obtained by iterating $\mathbf{v}^k = S^k S^{k-1} \cdots S^1 S^0 \mathbf{v}^0$ in place of (1).

The re-distribution of the particle densities at each discrete time step is accomplished according to prescribed rules that model the movement of the particle only along paths connecting adjacent nodes on the graph of the lattice. For example, a particle located at any node (i, j) in the interior of the 2D rectangular lattice has four directions in which

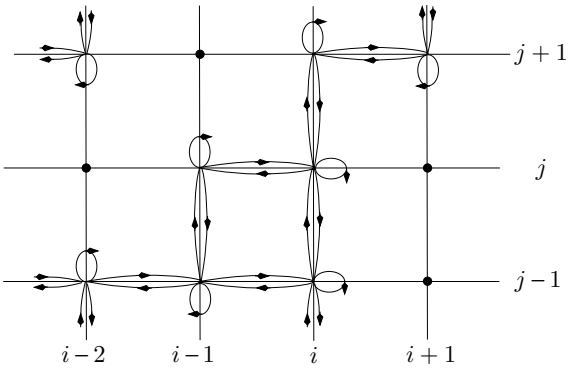

Figure 1. Typical regular Cartesian lattice onto which a connected graph of nodes and loops is imposed. The dark circles at the intersection of the coordinates signify inaccessible sites where impurities are located. Note that nodes adjacent to inaccessible sites have a loop, i.e., are re-entrant, and that each connecting edge has two pathways with one leading to each node and one leading away from each node.

to move associated with each of the Cartesian coordinate directions. The probability of each lattice node-to-node transition is then expressed for each node using the probabilities $P(i \to i-1, j) = P_E$, $P(i \to i+1, j) = P_W$, $P(i, j \to j+1) = P_N$, $P(i, j \to j-1) = P_S$, representing the four Cartesian directions. In the simplest case, these are uniformly the same throughout the medium. The influence of the external field favoring a directional bias is accounted for by specifying, e.g., $P_S > P_N$, to achieve a downward bias, whereas, lateral motion is typically taken to be isotropic, i.e., $P_E = P_W$.

A more realistic enhancement of this basic Cartesian model, used throughout this paper, includes obstacles representing nodes that are inaccessible to the particle, as shown in figure 1. In this case the transition probabilities of particles on nodes adjacent to the obstacle are adjusted so as to re-normalize the lattice motion through the use of an in-scatter probability in which the particle's motion is modeled as a loop. Thus in regard to the basic Cartesian model, each node has not four, but five transition probabilities associated with it. These now include P_I for the in-scatter probability satisfying $P_N + P_E + P_S + P_W + P_I = 1$. The addition of P_I allows the modeling of (1) obstacles, as well as (2) particle interactions, including stationary walks in which the particle remains inactive for a time step transition. The resulting graph is somewhat reminiscent of the transport graphs used in maximum flow problems, but in this case the link weights have nothing to do with capacities and cycles are allowed.

The transport medium is modeled to contain N_0 sites into which $n_i < N_0$ impurities are introduced to act as obstacles with $c_i = n_i/N_0$ being the impurity concentration. The corresponding graph consists of $N_0 - n_i$ vertices representing the remaining nodes, plus one representing a virtual source and one representing a virtual sink. These are added for computational convenience. In this construction no arc pointing toward the virtual source is allowed, and similarly all exiting sites are required to connect to the virtual sink, which contains a loop or in-scatter probability of 1, i.e., all particles accumulate at the sink. The dispersion of the initial distribution on the lattice is thus easily accomplished using a virtual source, and the collection of particles is similarly achieved at the virtual sink.

In this study all impurities acting as obstacles are assigned randomly to a starting or underlying lattice structure, and subsequently for computational efficiency nodes in the associated graph corresponding to nodes with impurities that have no edges connecting them with any other node, are eliminated—their rows and columns in the matrix, as described in (2),

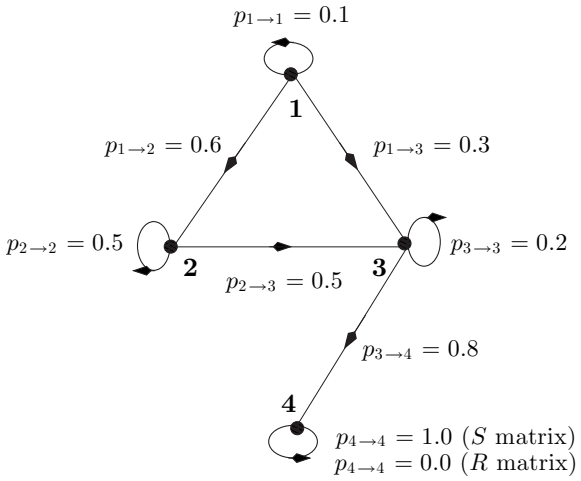

Figure 2. An example of a graph showing nodes, links and loops, along with the node to node transition probabilities. Note that the in-scatter probabilities are represented by the values of the loops at each node. In particular this simple example shows the use of a source node numbered 1 and sink node numbered 4.

are series of 0's anyway. Similarly, nodes which are completely surrounded by impurities are eliminated from the matrix; in the matrix they are recognizable by a diagonal (loop) coefficient equal to 1. Thus the initial graph is reduced to a smaller effective graph of size $N < N_0$ that describes only the remaining free vertices that are accessible by the particle. These free nodes may or may not form a connected cluster displaying at least one path from the source to the sink. Indeed, there is no reason to start with or use a Cartesian grid, as has been done, except computational simplicity, and a non-constant node connectivity can be considered.

Finally, the column stochastic matrix S is constructed based on the effective graph by assigning a sequential node numbering with coefficients consisting of the $N \times N$ values s_{ij} containing the discrete probabilities, i.e.,

$$s_{jk} = P(x_k \to x_j), \qquad 1 \leqslant j \leqslant N \quad \text{and} \quad 1 \leqslant k \leqslant N, \tag{2}$$

that is to say, the probability that a particle traverses from node x_k to node x_j in the lattice, where x_k and x_j are adjacent nodes. Since the numbering of the nodes is arbitrary it is convenient to label node 1 to be the virtual source and node N to be the virtual sink.

2.2. An elementary example

Consider the graph shown in figure 2 in which nodes 1–4 are connected so that particles flow from node 1 to 2, 1 to 3, 2 to 3 and 3 to 4, along with in-scattering loops at each node representing the probability that the particle stays at each node. While this example is not typical of the regular two-dimensional lattices examined in this work to model driven diffusion in media with impurities, it does contain two salient features not described in figure 1, namely the presence of single source and sink. Moreover, its simplicity allows for easy computation of the quantity of interest, i.e., the mean crossing time and its variance.

Construct $S = [s_{ij}]$, $i = 1, \ldots, 4$, $j = 1, \ldots, 4$ as the matrix of the graph modeling the nodal transitions in the driven diffusion problem. The dimension 4 of S is equal to the number

of sites in the medium plus the total number of virtual sources and sinks if any. Set each coefficient s_{ij} of S equal to the probability that link (j, i) is used by the particle when moving from j to i. The sink at vertex v_4 is characterized by assigning to this special site a loop with weight 1. The construction results in a matrix S that is column stochastic, i.e.,

$$S = \begin{pmatrix} 0.1 & 0.0 & 0.0 & 0.0 \\ 0.6 & 0.5 & 0.0 & 0.0 \\ 0.3 & 0.5 & 0.2 & 0.0 \\ 0.0 & 0.0 & 0.8 & 1.0 \end{pmatrix}.$$

Define a state vector $\mathbf{v}^k = \left[v_1^k, v_2^k, v_3^k, v_4^k\right]$ whose components $v_i^k, i = 1, \ldots, 4, k \geqslant 0$ represent the respective weights of the sites i in the lattice at discrete time $t_k = k$. Then, $\mathbf{v}^k = S\mathbf{v}^{k-1}, k \geqslant 0$. Initializing the state vector $\mathbf{v}^0 = [1, 0, 0, 0]$, vertex 1, i.e., v_1 has a full load and vertices 2–4 are empty. Of course, since S is column stochastic, $\|\mathbf{v}^k\|_1 = 1$ for all k. Iterating this system yields

$\mathbf{v}^1 = [0.1, 0.6, 0.3, 0]$,
$\mathbf{v}^2 = [0.01, 0.36, 0.39, 0.24]$,
$\mathbf{v}^3 = [0.001, 0.186, 0.261, 0.552]$,
$\vdots$
$\mathbf{v}^{10} = [1.0 \times 10^{-10}, 0.001\,464\,84, 0.002\,440\,69, 0.996\,094\,47]$,
$\vdots$
$\mathbf{v}^{50} = [1.0 \times 10^{-50}, 1.332\,27 \times 10^{-15}, 2.220\,45 \times 10^{-15}, 0.999\,999\,999\,999\,997]$,

where for notational clarity, the obvious transposition of row vectors is dropped. Focusing on the last component of each $\mathbf{v}^k$, corresponding to the weight of the sink (or exit site) of the graph, the density accumulates gradually such that all the weight contained initially in v_j^k, $j = 1, 2$ and 3 is transported to v_4^k.

The mean crossing time $\langle T \rangle$, i.e., the time required for all of the mass to exit the system at the sink, is defined as the weighted sum of the fraction of particles exiting in the time interval from $k-1$ to k times the time taken to exit, summed over all k. For the system under consideration the fraction accumulated at node 4 from time $k-1$ to k is $\left(v_4^k - v_4^{k-1}\right)/1$, hence

$$\langle T \rangle = \sum_{k=1}^{\infty} k\left(v_4^k - v_4^{k-1}\right). \tag{3}$$

Its variance is defined by

$$\sigma^2(T) = \langle T^2 \rangle - \langle T \rangle^2 = \sum_{k=1}^{\infty} k^2\left(v_4^k - v_4^{k-1}\right) - \langle T \rangle^2. \tag{4}$$

For the 4×4 system being discussed,

$$\langle T \rangle \approx 3.694\,444, \qquad \text{with} \quad \sigma^2(T) \approx 2.658\,179. \tag{5}$$

For comparison a Monte Carlo simulation of the driven diffusion process through the same medium requires 10^{12} independent random walks to obtain a six-digit accuracy for the mean value and variance of the crossing time.

2.3. A more tractable alternative

In contrast to section 2.2, consider the elimination of the loop at s_{44}, thus representing the sink vertex as an open node. At each time step the sink still collects the densities that are re-distributed to it, but this temporary collection will be lost at the next time step. At the sink component of the vector, i.e., at v_4 at time k, v_4^k represents the probability of the crossing time T for that component. The matrix obtained from S by setting a loop value at a sink equal to 0, is denoted as the R matrix associated with S. This corresponds to setting the value of the loop at the sink in figure 2 to zero, and thus R is a sub-stochastic column matrix.

In this example, this is given by

$$R = \begin{pmatrix} 0.1 & 0.0 & 0.0 & 0.0 \\ 0.6 & 0.5 & 0.0 & 0.0 \\ 0.3 & 0.5 & 0.2 & 0.0 \\ 0.0 & 0.0 & 0.8 & 0.0 \end{pmatrix},$$

so that the state vector $\mathbf{u}$, starting at $\mathbf{u}^0 = \mathbf{v}^0$, evolves in time as

$$\begin{aligned} \mathbf{u}^1 &= [0.1, 0.6, 0.3, 0.], \\ \mathbf{u}^2 &= [0.01, 0.36, 0, 39, 0.24.], \\ \mathbf{u}^3 &= [0.001, 0.186, 0.261, 0.312], \\ &\vdots \\ \mathbf{u}^{10} &= [1.0^{-10}, 0.001\,464\,84, 0.002\,440\,69, 0.003\,903\,39], \\ &\vdots \\ \mathbf{u}^{50} &= [1.0 \times 10^{-50}, 1.332\,27 \times 10^{-15}, 2.220\,45 \times 10^{-15}, 0.355\,271 \times 10^{-14}]. \end{aligned}$$

The mean crossing time, $\langle T \rangle$, in this modified model is given by summing the fraction of the mass crossing vertex 4 at each time step multiplied by the time, k, taken for the mass to reach exit node 4, i.e.,

$$\langle T \rangle = \sum_{k=1}^{\infty} k u_4^k. \tag{6}$$

In the case being modeled, there is only one exit node at 4. Since all rows except the last row of matrices S and R are zero in the last column, iterating the matrices, i.e., computing S^k and R^k yields the same results except for possibly the coefficients in the last row where the iterated matrices may differ. In this case, since $s_{44}^k = 1$ for all k, the transition from S^{k-1} to S^k, i.e., computing $S(S^{k-1})$, adds an extra copy of s_{4j} to the fourth row and jth entry of S^k compared to the corresponding coefficient entries in R^k. Thus,

$$r_{4j}^k = s_{4j}^k - s_{4j}^{k-1}, \qquad \text{for} \quad j = 1, 2, 3, 4, \tag{7}$$

where r_{ij}^k and s_{ij}^k are the coefficient entries of R^k and S^k, respectively. Note that this correctly shows that $r_{44}^k = 0$ for all k. Moreover, this shows that the mean crossing time $\langle T \rangle$ defined in (6) is the same as that defined in (3) since v_4^k can be computed from $R^k\mathbf{u}^0$ or from $(S^k - S^{k-1})\mathbf{v}^0$. Inspecting the partial sums in (6) shows that the numerical values settles at 3.694 444, consistent with the previously obtained result.

3. Computing mean crossing times

Consider the general $N \times N$ transition matrix S modeling driven diffusion on N free nodes, for which node N is the virtual sink for all of the nodes. Then $s_{NN} = 1$ and the related matrix

R has $r_{NN} = 0$. Going back to the expression in (6), this can be considered as the by-product of a more general expression involving the state vector $\mathbf{u}$,

$$\langle \mathbf{x} \rangle = \sum_{k=1}^{\infty} k\mathbf{u}^k \tag{8}$$

in which the components of $\mathbf{x}$ are identified with $\langle T \rangle$. Expanding the sum in (8),

$$\begin{aligned}\langle \mathbf{x} \rangle &= \mathbf{u}^1 + 2\mathbf{u}^2 + \cdots + k\mathbf{u}^k + \cdots \\ &= R\mathbf{u}^0 + 2R^2\mathbf{u}^0 + \cdots + kR^k\mathbf{u}^0 + \cdots \\ &= (R + 2R^2 + 3R^3 + \cdots + kR^k + \cdots)\mathbf{u}^0 \\ &= \sum_{k=1}^{\infty} kR^k\mathbf{u}^0. \end{aligned} \tag{9}$$

The matrix sum to left of $\mathbf{u}^0$ in (9) is isomorphic with sum of scalar variables, $\sum_{k=1}^{\infty} kx^k = x/(1-x)^2$ for $|x| < 1$, and so it is evident that the matrix sum in (9) can be obtained from

$$(I - R)^2(R + 2R^2 + 3R^3 + \cdots + kR^{k-1} + \cdots) = R - kR^k + (k-1)R^{k+1}. \tag{10}$$

Due to the structure of R, i.e., the last column consisting entirely of zeros, $\lim_{k\to 0} R^k = 0$, hence (10) reduces on the right to R for k going to infinity. Note that the invertibility of $(I - R)$, where I is the $N \times N$ identity matrix, is physically justifiable provided that the vertices of R contain at least one edge path connected from the virtual source to sink, however sufficient conditions are provided at the end of this section, along with a more detailed discussion of this in section 7.2.

Thus the value of the infinite matrix sum at the left of $\mathbf{u}^0$ in (9) reduces to

$$U = R((I - R)^2)^{-1},$$

so that $\langle \mathbf{x} \rangle = U\mathbf{u}^0$. Since the virtual sink is numbered as the last node in the graph, denote the sink component of a vector $\mathbf{x} = [x_1, x_2, \ldots, x_N]$ by $[\mathbf{x}]_N \equiv x_N$. Thus,

$$\langle T \rangle = [U\mathbf{u}^0]_N. \tag{11}$$

In a similar way the variance of T is evaluated using the expression

$$\sigma^2(T) = \langle T(T-1) \rangle + \langle T \rangle - (\langle T \rangle)^2 \tag{12}$$

in which

$$\begin{aligned}\langle T(T-1) \rangle &= \sum_{k=1}^{\infty} k(k-1)[\mathbf{u}^k]_N, \\ &= [\{2R^2 + 6R^3 + 12R^4 + \cdots + k(k-1)R^k + \cdots\}\mathbf{u}^0]_N, \\ &= [\{2R^2((I - R)^{-1})^3\}\mathbf{u}^0]_N. \end{aligned} \tag{13}$$

Using (11) and (12), along with (13), it is possible to compute the mean crossing time and the variance of the mean crossing time exactly, although at the expense of computing the inverse of the matrix $I - R$.

Going back to the example in (2.3),

$$(I - R)^{-1} = \begin{pmatrix} 10/9 & 0 & 0 & 0 \\ 4/3 & 2 & 0 & 0 \\ 5/4 & 5/4 & 5/4 & 0 \\ 1 & 1 & 1 & 1 \end{pmatrix},$$

$$U = R((I-R)^{-1})^2 = \begin{pmatrix} 10/81 & 0 & 0 & 0 \\ 76/27 & 2 & 0 & 0 \\ 485/144 & 45/16 & 5/16 & 0 \\ 133/36 & 13/4 & 5/4 & 0 \end{pmatrix},$$

with $\langle \mathbf{x} \rangle = U\mathbf{u}^0 = [10/81, 76/27, 485/144, 133/36]$ and $\langle T \rangle = x_4 = 133/36 = 3.694\,444$. Finally,

$$Z = 2R^2((I-R)^{-1})^3 = \begin{pmatrix} 20/729 & 0 & 0 & 0 \\ 1448/243 & 4 & 0 & 0 \\ 23\,405/2592 & 205/32 & 5/32 & 0 \\ 8173/648 & 77/8 & 5/8 & 0 \end{pmatrix}.$$

Hence, $Z\mathbf{u}^0 = (20/729, 1448/243, 23\,405/2592, 8173/648)$ and $\langle T(T-1) \rangle$, with sink component $[Z\mathbf{u}^0]_4 = 8173/648$, so that $\sigma^2(T) = \langle T(T-1) \rangle + \langle T \rangle - (\langle T \rangle)^2 = 3445/1296 = 2.658\,179$.

Both $\langle T \rangle$ and $\sigma^2(T)$ obtained using (11) and (13), respectively, are of course equal to the values found in section 2.3, but the apparent complications introduced by the matrix operations are more than well compensated by the degree of the numerical accuracy, mainly due to the fact that the series are not truncated.

Let λ be an eigenvalue of R. Since $|\lambda| \leqslant \|R\|_1 = 1$, R can have eigenvalues on the unit circle. Note that if the spectral radius, $\rho(R)$, lies on the unit circle, the corresponding eigenvector describes a stationary state of the system. The non-zero components of this vector represent the weights trapped at the corresponding sites of the lattice. Therefore some of the initial load (possibly all of it) is not able to reach the sink, and the notion of crossing time becomes meaningless, or alternatively, the mean crossing time becomes infinite. As will be shown in section 7.2, this behavior can be quite complex, yielding matrices whose largest eigenvalues are one, and yet those for which the transport of particles follows an exponential decay.

The matrix R is not an irreducible matrix as the graph of R cannot be strongly connected, at the very least because of nodes 1 and N. Since R contains all zeros in its last column, there is no vector $\mathbf{x}$ such that $R\mathbf{x} = \lambda\mathbf{x}$, consequently by the Perron–Frobenius theorem, $R \geqslant 0$ cannot be irreducible. In general the stochastic matrix S can be seen to be an irreducible primitive matrix for problems involving a regular lattice, such as in figure 1, provided that the none of the node-to-node transition probabilities completely vanishes.

The invertibility of $(I - R)$, whenever the largest eigenvalue of R is less than one, is easily established using M-matrices in the case when there are no impurities. M-matrices are non-singular matrices whose off-diagonal coefficients are non-positive, and whose inverses are non-negative. Equivalently, a matrix A is said to be an M-matrix if and only if there is a matrix $B \geqslant 0$ and $r > \rho(B)$ such that $A = rI - B$. Substituting $I - R$ for A, and using $r = 1$, since $\rho(R) < 1$ in the cases of interest, we have that $(I - R)$ is an M-Matrix if and only if there exists $R \geqslant 0$ and $1 > \rho(R)$ such that $I - R = 1 \cdot I - R$. Thus, $I - R$ is an M-matrix, and so $(I - R)^{-1} \geqslant 0$.

That R has eigenvalues less than 1 when there are no impurities follows from examining the $(N-1) \times (N-1)$ block matrix that excludes the last row of R. Denote this matrix as $R_{N-1,N-1}$, and observe that the eigenvalues of $R_{N-1,N-1}$ are the same as for R since a co-factor expansion of the determinant of R along this last column contributes nothing to the determinant of R. When there are no impurities, every entry in row N of R is non-negative. Hence, each column of $R_{N-1,N-1}$ necessarily sums to less than 1, hence $|\lambda| \leqslant \|R_{N-1,N-1}\| < 1$. This means that the eigenvalues of R are also strictly less than 1, demonstrating that the computation

of the means crossing time and its variance can always be accomplished as given in (11) and (13). The case with impurities is somewhat more complicated, and is discussed in section 7.1.

Finally, this last point requires some elaboration. Clearly, if the passage through the medium is blocked so that there is at least one node that fails to connect to the sink at node N, then that column of the matrix of $R_{N-1,N-1}$ must sum to 1, instead of summing to less than 1. In this case the eigenvalues of $R_{N-1,N-1}$ may equal to 1 exactly, and it is no longer possible to bound the eigenvalues of $R_{N-1,N-1}$, and hence of R, to be strictly less than 1. This means that $(I - R)$ may not be invertible, despite the presence of a conducting path from source to sink.

4. The case of interacting particles

The previous studies have assumed that the particles do not interact, or alternatively that there is a single particle. This is too restrictive since for many physical problems when the number of particles is large, as a particle is about to move, it frequently meets another particle located at the destination it had chosen, preventing it from moving, much like an impurity would; and the higher the number of particles, the larger the probability of such a blocking event. Since the lattice graph model does not represent the particles directly, the mechanism for modeling particle interaction is through a modification of the weights assigned to the in-scatter loops of the graph.

Constructing an accurate model may require modifying the underlying matrix coefficients at each node in time. While the time step dependence can be accounted for, local modifications of the coefficients would make the matrix method intractable in regard to estimating the mean crossing time. Thus examining the effects of non-local modifications that take into account the updates at each step, k, the most general form consists of

$$S_k = f_k(S), \tag{14}$$

where $S = S_0$ and f_k is a positive function of k that preserves the stochasticity of S_k for all k. Clearly, the modification of the matrices S_k depends on the physics of the particle–particle interactions, however there are some generic models that provide insight into particle interactions that are worth examining.

In the case of a high density of particles, choosing f_k as a homotopy between the stochastic matrix S and the identity matrix, i.e.,

$$S_k = x^k S_0 + (1 - x^k) I, \qquad 0 < x < 1, \tag{15}$$

satisfies these requirements. The role of x is perhaps more visible in the recursion relation that generates (15),

$$S_k = x S_{k-1} + (1 - x) I. \tag{16}$$

Applying the coefficient x at each time step reduces the weights of any free links, while simultaneously increasing the weights of the in-scatter loops. The effect is a re-distribution, i.e., the net losses and gains are equal so that the matrix remains column stochastic. Furthermore, since S and I commute, all of matrices commute at any time step k_1 and k_2, i.e., $S_{k_1} S_{k_2} = S_{k_2} S_{k_1}$.

Starting from an initial state $\mathbf{v}^0$ of the system, the iteration is given by

$$\mathbf{v}^1 = S_1 \mathbf{v}^0, \qquad \mathbf{v}^2 = S_2 \mathbf{v}^1, \qquad \ldots, \qquad \mathbf{v}^k = S_k \mathbf{v}^{k-1}, \tag{17}$$

so that the successive states of the system are given by $\mathbf{v}^k = \prod_{l=1}^{k} S_l \mathbf{v}^0$, and again as in section 2.2

$$\mathbf{u}^k = \mathbf{v}^k - \mathbf{v}^{k-1} = \left(\prod_{l=1}^{k} S_l - \prod_{l=1}^{k-1} S_l \right) \mathbf{v}^0 \tag{18}$$

represents the weight increment of $\mathbf{v}$ when going from $k-1$ to k, but S^k of section 2.2 is now replaced by $\prod_{l=1}^{k} S_l$. The evaluation of $\langle T \rangle$ is similar to the procedure in (3) and consists of evaluating

$$\langle T \rangle = \left[\sum_{k=1}^{\infty} k\mathbf{u}^k \right]_N . \tag{19}$$

The structure of the R matrices is analogous to that of the S matrices, except that their expression is given by

$$R_k = x^k R_0 + (1 - x^k) J, \tag{20}$$

where J is the matrix obtained from the identity matrix by setting the sink diagonal term equal to 0. Contrary to the S_k matrices, the R_k matrices no longer commute, however this does not matter because there is no 'inverse matrix' formalism for obtaining the mean crossing time and its variance directly. Using the R matrices to obtain $\langle T \rangle$, i.e., constructing $\mathbf{u}^k = \prod_{l=1}^{k} R_l \mathbf{u}^0$ is, however, computationally slightly advantageous over using the S matrices.

The homotopy given in (15) results in a 'freezing' of the lattice transport with increasing time since as $k \to \infty$ $S_k \to I$, i.e., all of the node-to-node transition probabilities become in-scattering loops. Reversing the role of x^k and $(1 - x^k)$ in (15), i.e.,

$$S_k = (1 - x^k) S_0 + x^k I, \qquad 0 < x < 1, \tag{21}$$

models an initial transient in which a large number of particles initially interact heavily, but later rarely interact. Finally, the homotopy model allows the modeling of transport in a system that is transitioning from an initial state, S_a to a final state S_b,

$$S_k = x^k S_a + (1 - x^k) S_b, \qquad 0 < x < 1. \tag{22}$$

Since S_a and S_b are stochastic, their convex sum is stochastic, but S_a and S_b do not necessarily commute.

5. Reductions to computable cases: accounting for collisions

The main handicap displayed in the previous section is the practical impossibility of performing the burdensome step-by-step summations needed in the evaluation of $\langle T \rangle$. At the cost of some accuracy we can adopt a simplified formalism in which the weights of the loop are constant in the process, so that (20) and (21) become

$$S(x) = xS + (1 - x) I \tag{23}$$

$$R(x) = xR + (1 - x) J \tag{24}$$

for some satisfactory values for the parameter x.

Consider, in the sample, the connected cluster of free sites on which particles can propagate from the source to the sink. When the particles attempt to move along the edges of that cluster in which original impurities are absent, there may be collisions every time several particles elect the same site in their move. In that case, one of the particles makes the move and plays the role of an impurity for the others. Assuming the moves to be isotropic, if several particles were free to occupy the same site, what is the fraction of the sites where more than one particle is present?

In the case of an infinitely large medium, the probability for a given site being occupied by k particles can be modeled using a Poisson law with parameter M, where M is the ratio of the number of particles N_w to the number of sites in the conducting cluster N,

$$Pr\{X = k\} = \mathrm{e}^{-M} M^k k!. \tag{25}$$

Table 1. Simulations of collisions on a 50×50 homogeneous lattice with two-dimensional periodic boundary conditions to simulate an infinite medium. There is excellent agreement with the simulated and theoretically computed collision densities for $X = 0$ (no collisions) and $X = 1$ (a single collision). The probability of multiple collisions is then given by (26). The statistics for the mean occupation rate per site is displayed as a pair consisting of the analytical value (25), and the value observed through simulation with 500 000 time steps.

	$Pr\{X = 0\}$		$Pr\{X = 1\}$	
M	Analytical	Simulation	Analytical	Simulation
0.048	0.953 134	0.953 129	0.045 7504	0.045 7605
0.3	0.740 818	0.740 776	0.222 2450	0.222 3170
0.6	0.548 812	0.548 737	0.329 2870	0.329 3880
0.9	0.406 570	0.406 524	0.365 913	0.365 9540
1.2	0.301 194	0.301 114	0.361 433	0.361 500

Simulations have been performed on square lattices of various sizes with periodic boundary conditions to evaluate the validity of computing the collision density using this Poisson model. In these studies, the medium is impurity free, just as the conducting cluster in the physical medium, and the particles are represented by points whose possible elementary moves are equally probable. The multiple in-scattering of the physical problem is represented by having several particles occupy the same site. The probability of multiple occupancy, $\mathcal{P}_m$, is given by

$$\mathcal{P}_m = 1 - Pr\{X = 0\} - Pr\{X = 1\} \tag{26}$$

$$= 1 - \mathrm{e}^{-M}(1 + M). \tag{27}$$

This is precisely the weight of the extra loop to be created at every site of the conducting cluster which had no loop before, and this weight can immediately be identified with the quantity $(1-x)$ in $R(x)$ or $S(x)$ in (23) and (24). For the sites which already had a loop before with a weight of R_{ii} on the diagonal of the matrix R, the new value is now $xR_{ii} + (1 - x)$ and the increase of the value is $(1 - x)(1 - R_{ii})$. The updating of the coefficients of R also applies to non-conducting sites but it does not matter since these sites do not participate in the conducting process.

The validity of the Poisson law even for a small sample is confirmed by the results of simulations performed on a square lattice at the vertices of which a certain number of particles have been placed. At each time step every particle is free to move with equal probabilities to any of its nearest or next-nearest neighbors, whether the elected site is already occupied or not. The results are shown in table 1. The two numbers within each parentheses are practically identical, justifying the use of a Poisson law to infer the multiple collision for the in-scattering process.

In the transport process the density of particles decreases with time due to the fact that more and more of them escape through the sink until eventually all of them have crossed the domain. Moreover, the density of particles in the sample during the dynamical process of traveling through the sample is not uniform and it is certainly incorrect to use only one global variable such as x to describe with accuracy the dynamics of the particles, however this simplification allows the reduction of the problem of the mean crossing time to be caste in a elementary analytical form, as will be shown. Most importantly, at low particle densities, the analytical simplification is justifiable. From table 1 and from figure 3 we can infer that, up to values of $M \approx 0.36$, the fraction of particles attempting multiple occupation of sites remains less than 0.05 and thus the method is applicable.

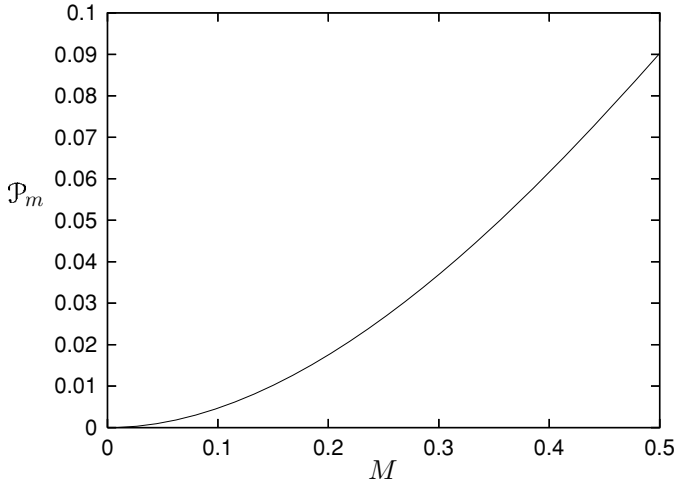

Figure 3. Probability of multiple collisions, $\mathcal{P}_m$, at a site using the Poisson probability density function as defined in (27). Observe that even for relatively large values of M, the value of $\mathcal{P}_m$ is quite small due to the parabolic nature of the curve near the origin, i.e., $\mathcal{P}_m \approx M^2/2$.

6. The uniformly scaled matrix

Consider the scaling of the reduced matrix R so that the in-scatter loops are increased by a factor $1 - x$ while scaling all of the off-diagonal terms governing the transport through the medium by x. Thus, continuing with the development of (20),

$$\tilde{R} \equiv R(x) = xR + (1 - x)J, \tag{28}$$

where $0 < x < 1$, and where $\tilde{R}$ is used for convenience to avoid the awkward functional dependence of R on x. Since the matrix R only has zero entries in column n, the matrix $\tilde{R}$ only has zero entries in column n. The mean crossing time, given the transition matrix R and the initial vector $\mathbf{u}^0$, can be calculated by evaluating the last term in the vector $R(I - R)^2\mathbf{u}^0$, i.e., $[R(I - R)^2\mathbf{u}^0]_n$, while the mean crossing time using the transition matrix $\tilde{R}$ is given by $[\tilde{R}(I-\tilde{R})^{-2}\mathbf{u}^0]_N$. In particular, the interest is in comparing $[\tilde{R}(I-\tilde{R})^{-2}\mathbf{u}^0]_N/[R(I-R)^{-2}\mathbf{u}^0]_n$, to determine the effects on the mean crossing time modifying the in-scattering due to multiple collisions. The assertion is that

$$[\tilde{R}(I - \tilde{R})^{-2}\mathbf{u}^0]_N/[R(I - R)^{-2}\mathbf{u}^0]_N = x. \tag{29}$$

The demonstration of this result follows from simple observation that

$$[\tilde{R}\mathbf{y}]_N/[R\mathbf{y}]_N = x \tag{30}$$

for any vector $\mathbf{y}$, while $(I-\tilde{R})^{-1}\mathbf{y}$ and $(I-R)^{-1}\mathbf{y}$ have exactly the same nth vector component, i.e.,

$$[(I - \tilde{R})^{-1}\mathbf{y}]_N/[(I - R)^{-1}\mathbf{y}]_N = 1, \tag{31}$$

hence that

$$[(I - \tilde{R})^{-2}\mathbf{y}]_N/[(I - R)^{-2}\mathbf{y}]_N = 1. \tag{32}$$

The proof of the scaling given in (30) follows from the fact that the last row of R and the last row of $\tilde{R}$ are exactly the same except that every entry of $r_{n,k}, k = 1, \ldots, N - 1$ of R

is scaled by x in $\tilde{R}$, except the last entry $r_{n,n}$ and $\tilde{r}_{n,n}$ which is zero in both matrices. Since the last entry of $R\mathbf{y}$ or $\tilde{R}\mathbf{y}$ is given by the dot product of this last row with $\mathbf{y}$, it follows that $x[R\mathbf{y}]_N = [\tilde{R}\mathbf{y}]_N$.

The evaluation of the comparison of $(I - R)^{-1}$ and $(I - \tilde{R})$ proceeds most easily if the matrices are block decomposed as

$$I - R = \begin{pmatrix} R_{N-1,N-1} & z_{N-1} \\ b_{N-1}^T & 1 \end{pmatrix}, \tag{33}$$

where $R_{N-1,N-1}$ is the $(N-1) \times (N-1)$ block matrix comprised of the first $N-1$ rows and first $n-1$ columns of R, z_N is the $N-1$ column vector consisting of all zeros, and b_{N-1}^T, the transpose of b_{N-1} is the $(N-1)$ row vector containing the first $N-1$ entries in the last row of R. From block multiplication, it is evident that the identity matrix I can be obtained from

$$I = \begin{pmatrix} R_{N-1,N-1}^{-1} & z_{N-1} \\ u_{N-1}^T & 1 \end{pmatrix} \begin{pmatrix} R_{N-1,N-1} & z_{N-1} \\ b_{N-1}^T & 1 \end{pmatrix}, \tag{34}$$

where u_{N-1}^T is the $(N-1)$ row vector containing all ones, corresponding to the bottom $1 \times (N-1)$ entries in the block matrix on the left-hand side of (34). It thus follows that

$$(I - R)^{-1} = \begin{pmatrix} R_{N-1,N-1}^{-1} & z_{N-1} \\ u_{N-1}^T & 1 \end{pmatrix}. \tag{35}$$

Note that this means that the bottom row of R^{-1} consists entirely of ones. The result in (34) is transparent except for the evaluation of the lower left block in which case it follows that

$$z_{N-1}^T = u_{N-1}^T R_{N-1,N-1} + b_{N-1}^T \tag{36}$$

since R is column stochastic in the first $N-1$ columns, hence $1 - R$ must have each of the first $N-1$ columns of R sum to zero. This is nothing other than the matrix product in (36). Using the same notation then, it follows that

$$I - \tilde{R} = \begin{pmatrix} xR_{N-1,N-1} & z_{N-1} \\ xb_{N-1}^T & 1 \end{pmatrix}, \tag{37}$$

hence that

$$(I - \tilde{R})^{-1} = \begin{pmatrix} xR_{N-1,N-1}^{-1} & z_{N-1} \\ u_{N-1}^T & 1 \end{pmatrix}. \tag{38}$$

Thus, whether the product $(I - R)^{-1}\mathbf{y}$ or the product $(I - \tilde{R})^{-1}\mathbf{y}$ is evaluated at the last term, the result is the dot product of the last row of either matrix, i.e, $(u_{N-1}, 1) = (u_N)$ with $\mathbf{y}$, and thus these are the same. Consequently, that the ratio of these terms is one has been demonstrated.

For the analysis of interest, i.e., the scaling of the mean transit time $\langle \tilde{T} \rangle$ as a result of replacing R with $\tilde{R}$, it is evident that this can be expressed concisely as

$$\langle \tilde{T} \rangle = \frac{1}{x} \langle T \rangle, \tag{39}$$

and so the effects on the mean crossing time of multiple collisions, at least in the limiting case of low densities, is seen to scale inversely proportionally with x. However, contrary to what might be expected, the higher cumulant $\sigma^2(\tilde{T})$ does not scale so elegantly with $1/x^2$. Referring back to table 1 and figure 3 in section 5, in which M has been identified with the density of particles on the conducting sites, this means for example, for $M = 0.4$, that $\mathcal{P}_m \approx 0.06$, and $x \approx 1 - 0.06 = 0.94$, consequently $\langle \tilde{T} \rangle \approx \langle T \rangle / 0.94 = 1.064 \langle T \rangle$.

7. Results and discussion

7.1. Computational studies

The model described in section 2.1 is applied to a square medium consisting 30×30 vertices with the purpose of examining the mean crossing times, $\langle T \rangle$, as a function of the directional (N–S) bias and the concentration of impurities. The graphs, after including a virtual source and a virtual sink, therefore have 902 vertices before the elimination of spurious vertices due to the addition of random impurities.

The iteration of the system is done using the R-matrices, and the computation of the mean crossing times is done using (12). Seven values of the relative bias P i.e., the relative weighting of downward motion to upward motion on the Cartesian grid are examined at a constant impurity concentration, and eight different impurity concentrations are used. The lateral motion is taken to be isotropic, and thus $\mathcal{P} = 1$ signifies a particle moving only down, while $P = 0$ signifies a particle moving only up in the medium, i.e., away from the sink.

The increase in the impurity concentrations is done using the same random seed for drawing the impurity sites, so that the set of impurities grows by inclusion and not by a complete re-distribution, thus yielding statistically correlated results. The plot of the mean crossing times is shown in figure 4 where the eight corresponding plots are $\log(\langle T \rangle)$ versus P, for the successive impurity concentrations, c_i: 0.20, 0.24, 0.27, 0.30, 0.35, 0.39 and 0.40. These results call for some comments:

(1) At each impurity concentration c_i, there is a P value for which $\langle T \rangle$ is minimum. This was qualitatively predictable, since a compromise has to exist between the slowing down of the particle movement at small values of P, i.e., $P \to 0$, while large values of P, i.e., $P \to 1$, makes P_N go to 0, discouraging any backward motion of the particle. Thus the particle can avoid obstacles due to impurities only by moving E or W, making its downward progression toward the sink more difficult. The minimum that is observed is in fact more accentuated than shows on the logarithmic plots in figure 4. The value of P at which the minimum occurs increases as the impurity concentration decreases, and goes to 1 in the absence of impurities, as it should.

(2) No results have been obtained for impurity concentration larger than 0.405 as the matrix inversion required in computing $\langle T \rangle$ fails, i.e., the matrix $I - R$ becomes singular. Since it is known that the critical site percolation threshold on a 2D square lattice corresponds to $c_i = 0.592$, representing the minimum concentration of active sites needed in order to observe a giant cluster that connects two opposite edges of a very large sample. This shows that the 30×30 lattice is too small, and as c_i increases it becomes increasingly probable that the particle lacks at least one path connecting the upper and the lower edges of the sample. Because of the small sample size, this occurs for $c_i > 0.495$, the value at which the random walk through the sample becomes impossible.

Finally, the homotopy model described in section 4 is applied using (15), and $\langle T \rangle$ is again of interest. Repeating the numerical studies using this variable model starting with x initially set to 1 and decreasing in steps of $1/100$, shows that $\langle T \rangle$ increases as x decreases up to the value $x = 0.88$, after which $\langle T \rangle$ decreases. This is unphysical, and a close check shows that although the norm of $\mathbf{v}^k$ as k increases remains equal to 1, as it should, the sink component does not go to 1 as the state vector is iterated.

Examining the components of $\mathbf{v}^k$, there are non-zero values everywhere, and thus the asymptotic state of the state vector $\mathbf{v}^k$ is frozen. This is consistent with the fact that as the term x^k modifying the weighting of the matrix S goes to 0, the matrix S_k approaches the identity,

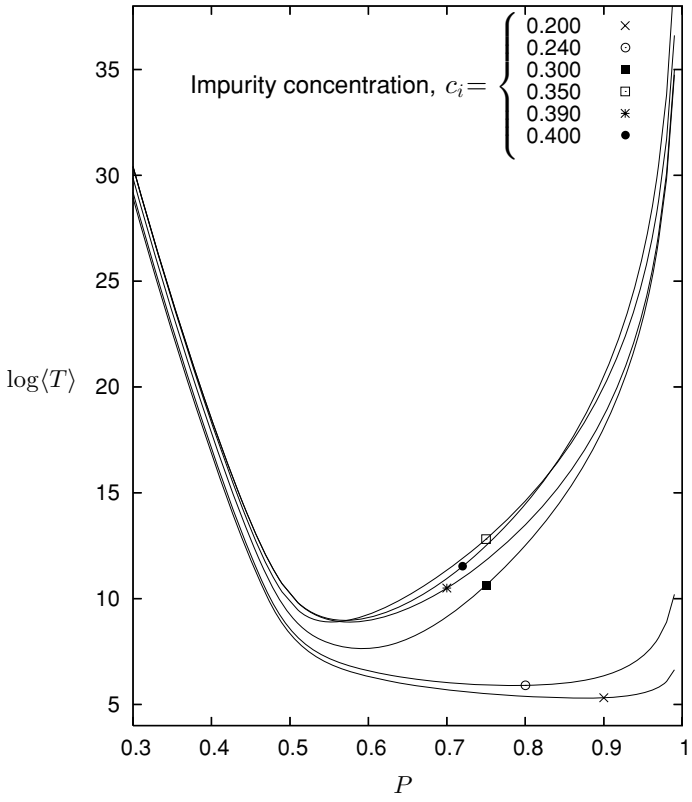

Figure 4. The logarithm of the mean crossing times, $\log\langle T\rangle$, for $x = 1$ as a function of the relative forward weighting of the particles' motions, P on a two-dimensional Cartesian grid. A value of $P = 0$ signifies that the particle has a relative probability 0 of moving downward in the direction of the sink, while 1 signifies that the probability of moving downward in the direction of the sink is 1. Note for $x < 1$, the mean crossing times are scaled by $1/x$, hence the curves shown are shifted up by $\log 1/x$. Note, the presence of a minimum associated with each value of c_i.

and thus all of the vertices contain only in-scattering loops. As a consequence part of the initial load does not reach the sink, thus making $\langle T\rangle$ infinite.

Interestingly, the larger the matrices, e.g., the 30×30 lattice, the more extreme the effect of x is, with the freezing of the state vector occurring for $x < x_c\, 0.9999$, where x_c denotes a critical value of x. The scaling of x_c on size of the lattice makes x a somewhat unrealistic variable to describe the processes, except perhaps giving an idea about how particles get trapped within the medium.

Clearly, the freezing is due to the rapidity with which $f(k) = x^k$ decreases with t, making all free bonds go too quickly to zero. One approach is to construct the function dependence $f(k) = (1 + bx^t)/(1 + b)$ where b is some positive adjustable constant, providing a reduction factor $1/(1 + b)$ to all free links as k goes to infinity and defining a new graph obtained from the initial graph through a re-normalization process. A second possibility consists in taking $f(k)$ as a slowly decaying function of k still going to zero for large k, such as a power law in k (for example $f(k) = 1/(1 + (k/a)^2)$); and, a third possibility is to realize that the dynamical effect created by multiple particles in the sample is not homogeneous through the sample, in

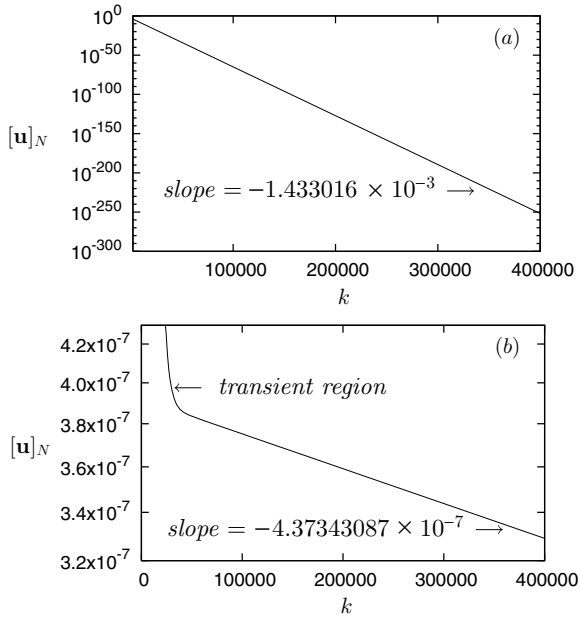

Figure 5. The density of particles at the sink as a function of the number of iterations k on a 20×20 matrix with (a) $p = 5/10$ with impurity concentration $= 0.0$, and (b) $p = 7/10$ with impurity concentration $= 0.39$. The medium has lateral re-entrant boundary conditions simulating a medium with infinite extent. Note the long transient region in (b) in contrast to (a) due to the high impurity concentration impeding transport from source to sink.

other terms, the weights of the links as k varies should also depend on the state vector $\mathbf{v}$. This leads to a nonlinear version of the problem which is presently beyond the scope of the present work.

7.2. The outflow process

While the interest is on computing the mean transit time of particles across the medium, this statistic does not fully describe the rate at which the system evolves due to the iteration of the sub-stochastic matrix R.

In considering the evolution of these systems, the examples provided in figure 5 are useful to examine in detail. In figure 5(a) the impurity to concentration is 0, i.e., there are no impurities randomly placed into the transport medium, and thus the movement of a particle from source node 1 to exit node N is unimpeded and driven only by the transition probabilities on the lattice. In this case there is no bias in the up–down movement, and still the particles exit rapidly. In contrast, in figure 5(b) the impurity concentration is 0.39 which is very close to the percolation threshold limit of the free sites in 2D for an infinite medium, i.e., the point at which the density of impurities randomly placed on the medium is likely to completely block passage from source to sink. The grid with impurities is shown in figure 6.

Referring to the matrix R associated with figure 5(a), the two largest eigenvalues of R are $\lambda_1 = 0.998\,568\,01$ and $\lambda_2 = -0.994\,415\,413$. Since $\lambda_1 < 1$, the matrix $I - R$ is invertible and the mean crossing time can be computed using (11). Equally of interest, the rate at which particles exit is seen to be an exponential decay, and the rate constant is seen to be equal to

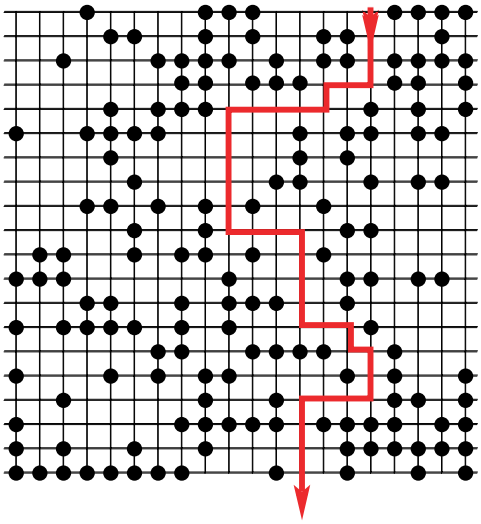

Figure 6. The lattice associated with the problem in figure 5(*b*). The virtual source and sink nodes are omitted from the diagram. Impurities are shown as black circles.

(This figure is in colour only in the electronic version)

$\log(\lambda_1) = -1.433\,016 \times 10^{-3}$. This is exactly the value obtained for the slope of the line, as can be expected in the case when a dominant eigenvalue λ_1 reduces the magnitude of its associated eigenvector by $\mathbf{e}_1$ at each iteration by R such that $\sum_{k=1}^{N} \alpha_k \lambda_k^n \mathbf{e}_k \approx \alpha_1 \lambda_1^n \mathbf{e}_1$. Thus $[\mathbf{u}_k]_N = [\mathbf{u}_0]_N \exp(-\lambda_1 k)$ represents the concentration of particles exiting at node N time step k.

The transport described in figure 5(*b*) also shows an exponential decay of the exiting particles after an initial transient. In this case, because of the impurities, it is difficult for the particles to reach the exit, and so it is reasonable to expect a delay in the initial crossing time. For this problem the two largest eigenvalues are given by $\lambda_1 = 1.0$ and $\lambda_2 = 0.999\,999\,562\,657\,0093$. The decay curve shown in figure 5(*b*) is consistent with the second largest eigenvalue, i.e., $\log(\lambda_2) = -4.373\,430\,863 \times 10^{-7}$ and the linear fit to the exponential decay for time steps larger than 100 000 yields a slope of $-4.373\,430\,87 \times 10^{-7}$. This is of significance, since the expectation would be that there is no transport on the medium given that $\lambda_1 = 1.0$.

To understand the governing process, it is necessary to examine the structure of the impurity distribution on the lattice that was used to obtain this result. Clearly, as seen in figure 6, the distribution of the impurities forms the walls of a maze through which the particles must travel, and in this case there is intrinsically only one conducting cluster from source to sink, i.e., from top to bottom in this figure. The path starting at node (1,16) exits only at node (20,14), having alternative exits as well at (20,10), (20,11) and (20,13). This conducting cluster accounts for the transmission rate through the medium, and the resulting exponential decay is characterized by λ_2.

In considering this result, it seems evident that the system consists, in effect, of two phases: one where the eigenvalue is $\lambda_1 = 1$, and the other where the eigenvalue is $\lambda_2 < 1$. But in fact, for the conducting phase, λ_2 is the largest eigenvalue and the long term diffusion of particles is described by this largest eigenvalue, as expected.

In contrast, λ_1 characterizes the existence of at least one blocking cluster which causes the medium to be partitioned into at least two sub-domains. Thus the existence of an eigenvalue equal to 1 for the matrix R corresponds to a strictly positive eigenvector describing a frozen distribution of particles located in a confined domain from which they cannot escape. Because the largest eigenvalue of R equals one, the matrix $I - R$ cannot be inverted, and thus in these type of problems the mean crossing time cannot be found using (11), however the mean crossing time obviously can always be obtained by directly summing the results as given by (6). This does come at a cost in computing time, particularly when the exponential curve exhibits a very slow decay as in figure 5.

It is important to realize that the results concerning the two phases apply to the results obtained in section 6 for multiple collisions where $\tilde{R} = R(x)$, as the homotopy preserves the ranking of the eigenvalues, i.e.,

$$\lambda_1(x) = x\lambda_1 + (1 - x) = 1, \tag{40}$$

$$\lambda_2 < \lambda_2(x) = x\lambda_2 + (1 - x) < 1, \tag{41}$$

where $\lambda_1(x)$ and $\lambda_2(x)$ are the eigenvalues of $R(x)$.

8. Conclusion

Modeling driven diffusion through the iteration of stochastic matrices which describe particle transition probabilities derived from the graph of a lattice provides an efficient alternative to simulation and Monte Carlo methods, and seems particularly suitable to parametric studies into which more or less physics can be introduced. Furthermore, the introduction of the in-scatter loops provides a mechanism for accounting for more complex phenomena than could be described using a traditional lattice model. The advantages of this approach, however, concern more than the computational aspects of driven diffusion problems, and the focus was on examining the analytical consequences of this approach, as well as on extracting some useful results that can be applied to characterize driven particle diffusion, e.g., the mean crossing time and its variance.

Whatever the deficiencies of the approach might be, the method is efficient and can be extended without restrictions to higher space dimensions and to a porous medium. In the latter case, the only significant change is that there is no longer a lattice and the number of neighbors accessible from a given site varies from site to site, so that the construction of the weighted graph describing the medium is tedious and requires a detailed inspection of the sites. Such a medium can be modeled by a distorted lattice where, after a random distribution of the impurities which in fact constitute the skeleton of the porous medium, the number and identity of the accessible neighbors to each site are now the result of a random drawing. The weights of the corresponding outgoing links should be such that not only do they sum up to 1, but they should incorporate a parameter accounting for a directional bias.

The extension from two to three dimensions may significantly increase the cost of 'inverting' the matrix $I - R$ for the mean crossing time and variance formulae, however since these matrices are all sparse, the efficient computation of these results along with the required matrix products is well developed, and can utilize parallel methods that can significantly reduce the computing costs. Thus, for example, while three dimensions means that for a $30 \times 30 \times 30$ lattice the matrix would be $27\,000 \times 27\,000$, problems of this size are well within the bounds for computationally evaluating $\langle T \rangle$ and $\langle T(T - 1) \rangle$ using (11) and (12).

There are reasons for selecting a linear iterative formulation. With S stochastic, the inversion of the operator is possible, allowing for the formulation of inverse problems in which

it may be possible to more fully correlate observation, i.e., transmittance of particles flowing through the material with the structural properties of the material. This includes solving the inverse problem associated with the structure of the matrix S itself, i.e., finding through optimization the best choice of coefficients for S which yield the observed experimental results. The approach also lends itself well to invariant embedding, i.e., where the lattice is modeled using sub-domains, each described by a matrix $S_{i,j}$ whose aggregate affects are modeled as a node in a larger matrix $\mathcal{S} = (S_{rs})$. Essentially $\mathcal{S}$ is a block matrix, which instead of being iterated directly, is iterated with the transition probabilities of each block being condensed to a single node. This approach would allow the modeling of complex, heterogeneous structures with large variabilities in constituents.

Acknowledgment

R Bidaux graciously acknowledges the assistance provided by the Department of Mathematics at the University of Southern Mississippi in support of this work.

References

[1] Chan T F, Kang S-H and Shen J 2002 Euler's elastica and curvature-based inpainting *SIAM J. Appl. Math.* **63** 564–92

[2] Chan T F and Shen J 2001 Non-texture inpainting by curvature-driven diffusion *J. Vis. Commun. Image Represent.* **12** 436–49

[3] Monthus C 2003 Localization properties of the anomalous diffusion phase $x \sim t^{\mu}$ in the directed trap model and in the Sinai diffusion with bias *Phys. Rev.* E **25** 046109

[4] Bidaux R and Pandey R B 1993 Driven diffusion of particles, first passage front and interface growth *Phys. Rev.* E **48** 2382

[5] Chunsheng L and Mai Y-W 2005 Influence of aspect ratio on barrier properties of polymer–clay nanocomposites *Phys. Rev. Lett.* **95** 1–4

[6] Schmittmann B and Zia R K P 1995 *Statistical Mechanics of Driven Diffusive Systems (Phase Transitions and Critical Phenomena* vol 17) (London: Academic)

[7] Walsh C A and Kozak J J 1982 Exact algorithms for d-dimensional walks on finite and infinite lattices with traps: II. General formulation and application to diffusion-controlled reactions *Phys. Rev.* B **26** 4166–89

[8] Gauthier M G and Slater G W 2002 Exactly solvable ogston model of gel electrophoresis: IX. Generalizing the lattice model to treat high field intensities *J. Chem. Phys.* **117** 6745–57